



Published in final edited form as:

*Mol Imaging*. 2008 ; 7(3): 147–152.

## Choline Autoradiography of Human Prostate Cancer Xenograft: Effect of Castration

Hossein Jadvar, Alparslan Gurbuz, Xiankui Li, Antranik Shahinian, and Peter S. Conti  
Molecular Imaging Center, Department of Radiology, University of Southern California, Los Angeles, CA

### Abstract

The purpose of this study was to investigate the effects of castration and tracer uptake time interval on the level of radiolabeled choline accumulation in murine-implanted human prostate tumor xenografts using quantitative autoradiography. We implanted androgen-dependent (CWR22) and androgen-independent (PC3) human prostate cancer cells in castrated ( $n = 9$ ) and noncastrated ( $n = 9$ ) athymic male mice and allowed tumors to grow to  $1 \text{ cm}^3$ . The mice were euthanized at 5, 10, and 20 minutes after injection of  $5 \mu\text{Ci}$  [ $^{14}\text{C}$ ]-choline. Mice were prepared for quantitative autoradiography with density light units of viable tumor sections converted to units of radioactivity ( $\text{nCi}/\text{mm}^2$ ) using calibration. Two-group comparisons were performed using a two-tailed Student *t*-test with unequal variance and with a significance probability level of less than .05. Two-group comparisons between the means of the tracer uptake level for each tumor type at each of three time points for each of two host types showed that (1) the level of tracer localization in the two tumor types was affected little in relation to the host type and (2) PC3 tumor uptake level tended to increase slowly with time only in the noncastrated host, whereas this was not observed in the castrated host or with CWR22 tumor in either host type. The uptake time interval and castration do not appear to significantly affect the level of radiolabeled choline uptake by the human prostate cancer xenograft.

---

*PROSTATE CANCER* is the most common cancer and thesecond leading cause of cancer death affecting men in the United States.<sup>1</sup> As life expectancy increases, so will the incidence of this disease, creating what may become an epidemic male health problem. As oncology departs from nonspecific diagnosis and treatment toward a “personalized” approach, accurate knowledge of the presence and extent of disease in combination with information on the physiologic, histologic, molecular, and genetic markers of the disease becomes crucially important.

The role of imaging in prostate cancer includes diagnosis of primary disease, determination of extracapsular spread, guidance and evaluation of local therapy in organ-confined disease, locoregional lymph node staging, detection of locally recurrent and metastatic disease during biochemical failure (prostate-specific antigen or PSA relapse), and assessment of tumor response to salvage and systemic therapy.<sup>2–4</sup> The current relatively limited experience with positron emission tomography (PET) with radiolabeled choline has shown that it may be useful in imaging prostate cancer in specific clinical situations.<sup>5–15</sup> The biologic basis for radiolabeled choline uptake in tumors is the malignancy-induced upregulation of choline kinase, which leads to the incorporation and trapping of choline in

the form of phosphatidylcholine (lecithin) in the tumor cell membrane in proportion to the rate of tumor duplication.<sup>16</sup>

Many questions remain before choline PET may be considered clinically, including the important consideration on how androgen (and androgen deprivation therapy) may affect the tumor uptake of radiolabeled choline. We therefore performed biodistribution and autoradiography studies of radiolabeled choline uptake in implanted androgen-sensitive and androgen-independent human prostate cancer mouse xenografts and investigated the effects of castration and uptake time interval on the level of [<sup>14</sup>C]-choline accumulation in the prostate tumor.

## Methods and Materials

We implanted androgen-sensitive (CWR22) and androgen-independent (PC3) human prostate cancer cells (American Type Culture Collection, Manassas, VA) at a concentration of  $10 \times 10^6$  cells per 0.2 mL in the shoulders and thighs, respectively, of 4- to 6-week-old, 20 to 30 g, castrated ( $n = 9$ ) and noncastrated ( $n = 9$ ) male athymic mice (BALB/c nu/nu), and the tumors were allowed to grow to 1 cm<sup>3</sup>. CWR-22 was derived from a human prostate carcinoma epithelial cell line derived from a xenograft that was serially propagated in mice after castration-induced regression and relapse of the parental, androgen-dependent CWR-22 xenograft. This cell line expresses PSA, and lysates are immunoreactive with androgen receptor antibody by Western blot analysis. The growth is stimulated by dihydroxytestosterone and epidermal growth factor. PC-3 was derived from bone metastasis of a grade IV prostate adenocarcinoma from a Caucasian male and exhibits low acid phosphatase and testosterone-5 $\alpha$ -reductase activities.

Castrated and noncastrated mice (Harlan Sprague-Dawley, Inc., Indianapolis, IN) served as models for the absence and presence, respectively, of androgens. No testosterone pellets or blood sampling was employed. Tumor volume was calculated using the formula  $S^2 \times L/2$ , where S and L represent the small and large diameters of the lesion. The lesion dimensions were measured using calipers at every 2- to 3-day interval. The CWR22 human prostate cancer cell line expresses androgen receptors and PSA and is stimulated by dihydroxytestosterone. The androgen-independent PC3 human prostate cancer cell line was initiated from a bone metastasis of a grade IV prostatic adenocarcinoma and displays low testosterone-5 $\alpha$ -reductase activity.

The mice were euthanized at 5, 10, and 20 minutes ( $n = 3$  mice per time point per group) after injection of 5  $\mu$ Ci [methyl-<sup>14</sup>C]-choline at specific activity of 55 mCi/mmol (MP Biochemicals, Inc., Irvine, CA). The mice were then prepared for quantitative autoradiography (Packard Instrument Company, Inc., Downers Grove, IL). The average density light units (*Optiquant* software) of the viable tumors (excluding necrotized photopenic areas) and major organs (brain, kidney, liver, muscle) were obtained from regions of interest over several image slices (range 6 to 18 slices at 50  $\mu$  per each slice) and then were converted to the units of radioactivity (normalized to injected activity and expressed in nCi/mm<sup>2</sup>) using calibration against a standard reference (Amersham Biosciences). Two-group comparisons were performed using a two-tailed Student *t*-test with unequal variance and with a significance probability level of less than .05.

All animal studies were approved by our Institutional Animal Care and Use Committee, the Biological Safety Committee, and the Radiation Safety Committee. Anesthesia was induced using one intraperitoneal injection of each of ketamine 80 mg/kg and xylazine 10 mg/kg, with an additional third of doses as needed. Euthanasia was by intraperitoneal injection of 120 mg/kg pentobarbital followed by cervical dislocation.

## Results

The tumors grew to about 1 cm<sup>3</sup> within 2 to 4 weeks after the implantation. The growth patterns of CWR22 tumor and PC3 tumor differed and were noted to be best approximated by an exponential function and a quadratic function, respectively, as was previously reported by our group.<sup>17</sup>

Biodistribution of [14C]-choline in major organs showed the highest uptake in the kidneys followed by that in the liver. Brain and skeletal muscle demonstrated substantially lower tracer localization. This pattern was maintained at the three time points of 5, 10, and 20 minutes after tracer administration despite some statistically insignificant fluctuations (Table 1). Additionally, there was no statistically significant difference in the major organ biodistribution patterns in relation to the two host types, suggesting that androgens do not affect the radiolabeled choline biodistribution significantly ( $p < .1$ ). Figure 1 shows a typical autoradiogram demonstrating the highest tracer localization in the kidneys and liver.

Figure 2 summarizes the two-group comparisons between the means of the tracer uptake levels for each tumor type at each of three time points for each of the two host types. The tracer localization in the two tumor types was affected little in relation to the host type, although there was a statistically significant difference between the means of tracer uptake in the two tumors at 10 minutes in the noncastrated host only. The PC3 tumor uptake level tended to increase slowly with time only in the noncastrated host, but this was not observed in the castrated host or with CWR22 tumor in either host type. There was also a statistically significant difference between the two host types in relation to the means of the tracer accumulation within the CWR22 tumor at only the 5-minute and 10-minute time points.

## Discussion

Prostate tumor uptake of choline is related to the upregulation of choline kinase, which leads to the incorporation and trapping of choline in the form of phosphatidylcholine in the tumor cell membrane in proportion to the rate of tumor duplication.<sup>16</sup> The tumor uptake level, however, does not appear to correlate with cellular proliferation (as depicted by Ki-67) or with clinical parameters such as PSA and Gleason sum score.<sup>18</sup> A recent report has shown that choline kinase expression in human prostate cancer may be regulated through the hypoxia-inducible factor-1 $\alpha$  signaling pathway, with the consequence of increasing cellular choline uptake in a hypoxic environment.<sup>19</sup> Interestingly, however, hypoxia may diminish choline uptake in both androgen-dependent and androgen-independent prostate tumors in contradistinction to an increase in tumor uptake of [18F]-fluorodeoxyglucose (FDG).<sup>20</sup>

Pilot human studies have shown that PET with [11C]-choline may be useful in the imaging evaluation of primary prostate cancer, for initial staging of disease, at the time of biochemical failure (PSA relapse) after curative primary treatment, and for restaging. One advantage of [11C]-choline over FDG is the negligible urinary accumulation of the tracer that can improve detection of the primary prostate tumor and local recurrence.<sup>5-15</sup> However, there can be significant overlap in the uptake levels of [11C]-choline in benign prostatic hyperplasia and in prostate cancer,<sup>21</sup> although a dual-phase imaging protocol (early and late) can potentially be helpful in differentiating benign tissue from malignancy,<sup>22</sup> but this notion has also been disputed by others.<sup>14</sup> In one study that compared the results of [11C]-choline PET-computed tomography (CT) with step-section histopathologic examination, a relatively high rate of false-negative PET-CT was found with a sensitivity of 66%, specificity of 81%, positive predictive value of 87%, and negative predictive value of 55%.<sup>23</sup> A relatively recent kinetic analysis of [11C]-choline with dynamic PET demonstrated that the influx constant  $K(i)$  and standardized uptake values correlated closely

( $r = .964$ ,  $p = .0005$ ), although there was overlap between the values for tumors and for a benign hyperplastic prostate. No correlation could also be demonstrated between the tumor uptake of [11C]-choline and the histologic grade, pathologic stage, Gleason sum score, and volume of the prostate or PSA.<sup>15,24</sup>

Initial findings with an F-18-labeled choline, [<sup>18</sup>F]fluoromethyl-dimethyl-2-hydroxyethyl-ammonium (FCH), has also indicated that FCH may also be useful in imaging of prostate cancer.<sup>25,26</sup> Tumor uptake of FCH was shown to be specific to choline transport and phosphorylation through inhibition studies with hemicholinium-3.<sup>27</sup> In vitro data have demonstrated higher FCH than FDG uptake in androgen-dependent (LNCaP) and androgen-independent (PC3) prostate cancer cells.<sup>28</sup> But, interestingly, the latter report also showed greater uptake of FDG than FCH in PC3 murine xenograft.<sup>28</sup> We also noted a similar finding when we compared our current results with choline autoradiography with those of our previously reported studies with FDG autoradiography of human prostate cancer mouse xenografts.<sup>17</sup> Early experience with pilot human studies has been encouraging in that FCH may be potentially useful in the imaging evaluation of prostate cancer.<sup>29</sup>

It appears that tumor accumulation of [11C]-choline differs among different prostate tumor types, which may be related to some underlying biologic process.<sup>30</sup> One important relevant biologic factor is the effect of androgen on the tumor uptake of radiolabeled choline. Hara and colleagues showed in an in vitro study that androgen depletion suppressed the uptake of [methyl-(3)H]-choline in an LNCaP androgen-dependent tumor, whereas it had no effect on the uptake level in a PC3 androgen-independent tumor.<sup>20</sup> In a small pilot human study, antiandrogen therapy was noted to reduce the FCH uptake in prostate cancer.<sup>27</sup> Similar observation has been made more recently with [11C]-choline in patients undergoing bicalutamide therapy.<sup>15</sup> However, in another recent report, antiandrogen therapy did not show a significant effect on the detection rate of [11C]-choline PET-CT.<sup>31</sup>

In one view, it may be beneficial if the tracer uptake is modulated by androgen since then androgen deprivation therapy may be assessed and there can be a potential possibility for predicting an impending androgen refractory state in castrated patients.<sup>17</sup> In another view, androgen dependence of tumor tracer uptake may adversely affect lesion detection sensitivity during androgen ablation therapy in specific clinical situations, such as during PSA relapse. Therefore, it is desirable to improve our understanding of how androgen therapy type, frequency, and duration affect the level of tracer uptake in prostate tumor.

The exact underlying biologic mechanism that relates the androgen effects to the uptake mechanism of choline radiotracers in the tumor remains unknown. However, as was recently suggested, androgen may induce a general enhancement of the cellular metabolism rather than a modulation of a specific biochemical pathway.<sup>20</sup> Given the current limited data and mixed results in relation to the effect of androgen on radiolabeled choline uptake in prostate cancer, we performed an animal model study of the spatiotemporal effects of androgen presence or absence on the level of [14C]-choline uptake in androgen-dependent and androgen-independent human prostate cancer xenografts and the overall biodistribution of the tracer. We employed a study of castrated and noncastrated mice to model the absence and presence of androgens that differs from the study by Price and colleagues, which used presumably noncastrated mice only.<sup>28</sup> In that study, testosterone pellets were implanted subcutaneously 72 hours prior to CWR22 injection into the mice flanks. In our study, we relied on the intrinsic androgen level in the noncastrated mice to model the physiologic condition to diminish the possibility of inducing nonphysiologic high androgen levels. Additionally, we sought to keep the experimental conditions similar between the castrated and noncastrated mice as implanting testosterone pellets in castrated mice would defy the intended castration effect. We also did not measure the plasma level of androgen in the

noncastrated mice as our study was not designed to address the potential modulatory effects of the varying levels of androgen, although such follow-up studies would be clearly helpful. Our results demonstrated a similar biodistribution of [14C]-choline, as has been observed with the pilot human [11C]-choline PET studies. Furthermore, our animal-based human prostate cancer xenograft study supports the findings of the very recent human-based [11C]-choline PET-CT study in that anti-androgen therapy may not have a significant effect on the tumor accumulation of radiolabeled choline. Our animal-based study also demonstrated that [14C]-choline accumulates in the prostate tumor early after tracer administration, which supports the very recent human-based finding that there may be little benefit with delayed imaging.<sup>14</sup>

Our general observations in animals should be considered in view of other potential modulating factors, such as tumor blood flow and hypoxia, which were not controlled in our study. Overall, the microvasculature, oxygenation distribution, and differences in the growth pattern of the xenograft tumors in comparison with those of the native spontaneous tumors may present additional varying effects on the results among studies.<sup>20,28</sup> An additional differing factor may be related to the selected time points in our study that was limited to 20 minutes that is more relevant to the human-based studies with C-11 choline (half-life of 20 minutes). Analysis of the tumor uptake level at longer time points (eg, 30, 60, and 90 minutes) after tracer administration may be more pertinent to F-18-labeled choline (half-life of 110 minutes), although one very recent study showed no clear benefit with a dual-phase protocol (3–5 minutes and 30 minutes) for the case of discriminating prostate bed malignancy from benign tissue.<sup>14</sup> In fact, another investigation has shown that maximal tumor uptake occurs at 4 minutes, with stable intensity over a time span of 20 minutes.<sup>27</sup> Nevertheless, additional systematic studies will be needed to establish the optimal imaging time for either C-11- or F-18-labeled choline in the imaging evaluation of prostate cancer.

In summary, our preliminary animal study reported here provides the foundation and is supportive of some of the recent observations with [11C]-choline PET in humans, which may help in further clarifying the current mixed results in literature. In general, however, additional animal-based and large prospective human studies are needed to define the exact role of various PET radiotracers, including radiolabeled choline, in specific clinical circumstances along the path of the natural history of prostate cancer.

## Acknowledgments

This work was supported by an award from The Wright Foundation and in part by National Institutes of Health–National Cancer Institute grant number R01-CA111613 to H. Jadvar.

## References

1. National Cancer Institute. SEER: The Surveillance, Epidemiology, and End Results program. Available at: <http://seer.cancer.gov>
2. Sanz G, Rioja J, Zudaire JJ, et al. PET and prostate cancer. *World J Urol.* 2004; 22:351–2. [PubMed: 15503049]
3. Hricak H, Choyke P, Eberhardt S, et al. Imaging prostate cancer: a multidisciplinary approach. *Radiology.* 2007; 243:28–53. [PubMed: 17392247]
4. Lawrentschuk N, Davis ID, Bolton DM, et al. Positron emission tomography and molecular imaging of the prostate: an update. *BJU Int.* 2006; 97:923–31. [PubMed: 16643472]
5. de Jong IJ, Pruijm J, Elsinga PH, et al. Visualization of prostate cancer with 11C-choline positron emission tomography. *Eur Urol.* 2002; 42:18–23. [PubMed: 12121724]
6. Picchio M, Messa C, Landoni C, et al. Value of [11C]choline-positron emission tomography for re-staging prostate cancer: a comparison with [18F]fluorodeoxyglucose-positron emission tomography. *J Urol.* 2003; 169:1337–40. [PubMed: 12629355]

7. Reske SN, Blumstein NM, Neumaier B, et al. Imaging prostate cancer with 11C-choline PET/CT. *J Nucl Med.* 2006; 47:1249–54. [PubMed: 16883001]
8. Martorana G, Schiavina R, Corti B, et al. 11C-Choline positron emission tomography/computerized tomography for tumor localization of primary prostate cancer in comparison with 12-core biopsy. *J Urol.* 2006; 176:954–60. [PubMed: 16890665]
9. Scher B, Seitz M, Albinger W, et al. Value of 11C-choline PET and PET/CT in patients with suspected prostate cancer. *Eur J Nucl Med Mol Imaging.* 2007; 34:45–53. [PubMed: 16932935]
10. Rinnab L, Mottaghy FM, Blumstein NM, et al. Evaluation of [11C]-choline positron-emission/computed tomography in patients with increasing prostate-specific antigen levels after primary treatment for prostate cancer. *BJU Int.* 2007; 100:786–93. [PubMed: 17822459]
11. Scattoni V, Picchio M, Suardi N, et al. Detection of lymph-node metastases with integrated [11C]choline PET/CT in patients with PSA failure after radical retropubic prostatectomy: results confirmed by open pelvic-retroperitoneal lymphadenectomy. *Eur Urol.* 2007; 52:423–9. [PubMed: 17397992]
12. Reske SN, Blumstein NM, Glatting G. [(11)C]choline PET/CT imaging in occult local relapse of prostate cancer after radical prostatectomy. *Eur J Nucl Med Mol Imaging.* 2008; 35:9–17. [PubMed: 17828534]
13. Husarik DB, Miralbell R, Dubs M, et al. Evaluation of [(18)F]-choline PET/CT for staging and restaging of prostate cancer. *Eur J Nucl Med Mol Imaging.* 2008; 35:253–63. [PubMed: 17926036]
14. Igerc L, Kohlfurst S, Gallowitsch HJ, Matschnig S, et al. The value of (18)F-choline PET/CT in patients with elevated PSA-level and negative prostate needle biopsy for localization of prostate cancer. *Eur J Nucl Med Mol Imaging.* 2008 [Epub ahead of print].
15. Giovacchini G, Picchio M, Coradeschi E, et al. [(11)C]Choline uptake with PET/CT for the initial diagnosis of prostate cancer: relation to PSA levels, tumor stage and anti-androgenic therapy. *Eur J Nucl Med Mol Imaging.* 2008 [Epub ahead of print].
16. Yoshimoto M, Waki A, Obata A, et al. Radiolabeled choline as a proliferation marker: comparison with radiolabeled acetate. *Nucl Med Biol.* 2004; 31:859–65. [PubMed: 15464387]
17. Jadvar H, Li X, Shahinian A, et al. Glucose metabolism of human prostate cancer mouse xenografts. *Mol Imaging.* 2005; 4:91–7. [PubMed: 16105512]
18. Breeuwsma AJ, Pruim J, Jongen MM, et al. In vivo uptake [11C]choline does not correlate with cell proliferation in human prostate cancer. *Eur J Nucl Med Mol Imaging.* 2005; 32:668–73. [PubMed: 15765234]
19. Glunde K, Shah T, Winnard PT Jr, et al. Hypoxia regulates choline kinase expression through hypoxia-inducible factor-1 alpha signaling in a human prostate cancer model. *Cancer Res.* 2008; 68:172–80. [PubMed: 18172309]
20. Hara T, Bansal A, DeGrado TR. Effect of hypoxia on the uptake of [methyl-3H]choline, [1–14C] acetate and [18F]FDG in cultured prostate cancer cells. *Nucl Med Biol.* 2006; 33:977–84. [PubMed: 17127170]
21. Yoshida S, Nakagomi K, Goto S, et al. 11C-Choline positron emission tomography in prostate cancer: primary staging and recurrent site staging. *Urol Int.* 2005; 74:214–20. [PubMed: 15812206]
22. Kwee SA, Coel MN, Lim J, et al. Prostate cancer localization with 18fluorine fluorocholine positron emission tomography. *J Urol.* 2005; 173:252–5. [PubMed: 15592091]
23. Farsad M, Schiavina R, Castellucci P, et al. Detection and localization of prostate cancer: correlation of (11)C-choline PET/CT with histopathologic step-section analysis. *J Nucl Med.* 2005; 46:1642–9. [PubMed: 16204714]
24. Sutinen E, Nurmi M, Roivainen A, et al. Kinetics of [(11)C]choline uptake in prostate cancer: a PET study. *Eur J Nucl Med Mol Imaging.* 2004; 31:317–24. [PubMed: 14628097]
25. DeGrado TR, Baldwin SW, Wang S, et al. Synthesis and evaluation of (18)F-labeled choline analogs as oncologic PET tracers. *J Nucl Med.* 2001; 42:1805–14. [PubMed: 11752077]
26. Heinisch M, Dirisamer A, Loidl W, et al. Positron emission tomography/computed tomography with F-18-fluorocholine for restaging of prostate cancer patients: meaningful at PSA<5 ng/mL? *Mol Imaging Biol.* 2006; 8:43–8. [PubMed: 16315004]

27. DeGrado TR, Coleman RE, Wang S, et al. Synthesis and evaluation of <sup>18</sup>F-labeled choline as an oncologic tracer for positron emission tomography: initial findings in prostate cancer. *Cancer Res.* 2001; 61:110–7. [PubMed: 11196147]
28. Price DT, Coleman RE, Liao RP, et al. Comparison of [<sup>18</sup>F]fluorocholine and [<sup>18</sup>F]fluorodeoxyglucose for positron emission tomography of androgen dependent and androgen independent prostate cancer. *J Urol.* 2002; 168:273–80. [PubMed: 12050555]
29. Kwee SA, Wei H, Sesterhenn I, et al. Localization of primary prostate cancer with dual-phase <sup>18</sup>F-fluorocholine PET. *J Nucl Med.* 2006; 47:262–9. [PubMed: 16455632]
30. Zheng QH, Gardner TA, Raikwar S, et al. [<sup>11</sup>C]Choline as a PET biomarker for assessment of prostate cancer tumor models. *Bioorg Med Chem.* 2004; 12:2887–93. [PubMed: 15142549]
31. Krause BJ, Souvatzoglou M, Tuncel M, et al. The detection rate of [(11)C]choline-PET/CT depends on the serum PSA-value in patients with biochemical recurrence of prostate cancer. *Eur J Nucl Med Mol Imaging.* 2008; 35:18–23. [PubMed: 17891394]

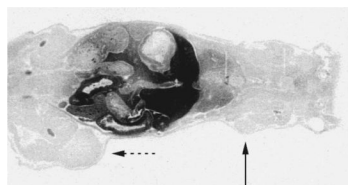


**Figure 1.** Typical autoradiogram demonstrating physiologic high tracer localization in the kidneys and the liver; androgen-dependent CWR22 tumor (*solid arrow*) and androgen-independent PC3 tumor (*dashed arrow*).



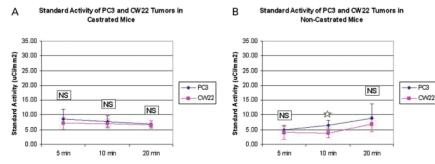


**Figure 2.** Tracer accumulation in the CWR22 and PC3 tumors in (A) castrated and (B) noncastrated hosts. NS 5 not significant. \* $p > .05$ .

**Table 1**Biodistribution of [<sup>14</sup>C]-Choline in Castrated and Noncastrated Athymic Male Mice (Mean ± SD)

<i>Castrated</i>	<i>5 min (n = 3)</i>	<i>10 min (n = 3)</i>	<i>20 min (n = 3)</i>
Kidney	274.1 ± 175.3	423.7 ± 146.6	232.2 ± 71.5
Liver	117.4 ± 16.7	156.2 ± 24.5	221.5 ± 48.3
Brain	13.4 ± 6.7	7.9 ± 2.5	10.1 ± 3.0
Muscle	8.5 ± 3.3	7.9 ± 3.0	7.0 ± 1.0
CWR22	7.2 ± 2.0	7.1 ± 1.5	6.7 ± 1.2
PC3	8.6 ± 3.4	7.7 ± 1.9	6.9 ± 1.0

<i>Noncastrated</i>	<i>5 min (n = 3)</i>	<i>10 min (n = 3)</i>	<i>20 min (n = 3)</i>
Kidney	402.9 ± 239.5	346.2 ± 248.2	259.6 ± 104.7
Liver	101.1 ± 24.0	113.6 ± 67.2	169.4 ± 98.5
Brain	9.7 ± 3.8	6.3 ± 1.7	5.7 ± 2.0
Muscle	8.9 ± 2.9	8.2 ± 0.8	6.5 ± 2.8
CWR22	4.1 ± 2.4	3.9 ± 1.7	6.8 ± 2.4
PC3	4.9 ± 1.3	6.5 ± 1.7	9.0 ± 4.7

Two-group comparisons were not statistically significant.